

# Gradient Pattern Analysis of Extended Convection-Diffusion

A.P.Mattedi R.R. Rosa

F.M. Ramos N.L. Vijaykumar  
Nucleous for Simulation and Analysis of  
Complex Systems (NUSASC), Lab for  
Computing and Applied Mathematics,  
National Institute for Space Research  
(INPE), C.P. 515, São José dos Campos -  
SP, 12201-970, Brazil.

J.A. Valdivia

Department of Physics, Facultad  
de Ciencias, Universidad de  
Chile, Casilla 653, Santiago,  
Chile.

A.S. Sharma

Department of Physics and  
Astronomy, University of  
Maryland, College Park, MD,  
USA.

## Abstract

In this paper we perform gradient pattern analysis (GPA) of convection diffusion given by the solution of 2D Burgers' equation. GPA leads to characterize initial condition coherence and spatio-temporal pattern equilibrium through the local/global averaging by using two different matrix computational operators: the Asymmetric Amplitude Fragmentation (AAF) and the Complex Entropic Form (CEF). The transport phenomenon is discussed in terms of its dependence to the initial condition distribution. The initial condition variability is given by a set composed by Gaussian and non-Gaussian distributions. The results have shown that the GPA is able to characterize different spatio-temporal nonlinear diffusion regimes.

Key words: gradient pattern analysis, Burgers' equation, anomalous diffusion.

## 1. Introduction

The gradient pattern analysis [1-4] is a geometrical approach to characterize formation and evolution of two-dimensional spatio-temporal patterns in extended nonlinear systems. Usually pattern formation in continuous extended systems is described by means of nonlinear interaction of plane waves. However, another approach to the problem of pattern formation is to identify robust structural properties for a single spatio-temporal wave. It has been shown in numerical simulations that the dynamical pattern of a single non-linear wave transport, in the physical space, carries a memory of its initial condition [4].

In nonlinear waves, competition occurs between two opposing processes: steeping, due to nonlinearity, and damping due to viscosity. The most fundamental equation to describe this dynamics is the so-called Burgers' equation for 1D, introduced by J. M. Burgers in 1940:

$$U_t + UU_x = \varepsilon U_{xx},$$

where  $U_i$  and  $x$  are amplitudes in the correspondent phase space, with  $U = f(x, t)$ , and  $\varepsilon$  is the coefficient of viscosity. A remarkable feature of Burgers equation is the existence of an exact solution, found by Cole in 1951. The exact solution reveals that there is a overturning instant  $t_0$  when  $\varepsilon = 0$ . If  $\varepsilon \neq 0$ , for  $t < t_0$  the steepness of the front increases, and so, does the derivative  $U(x, t)$ . As a result of this, even for small viscosities, the term  $\varepsilon U_{xx}$  on the right-hand side of the equation becomes large and matches the convective term  $UU_x$ . The central difference approximation for the Burgers' equation in two-dimensions is [12]:

$$U_{i,j}^{n+1} - U_{i,j}^n = \left( \frac{\varepsilon \Delta t}{\Delta x^2} \right) \delta_x^2 U_{i,j}^n + \left( \frac{\varepsilon \Delta t}{\Delta y^2} \right) \delta_y^2 U_{i,j}^n - \left( \frac{\Delta t}{2\Delta x} \right) \delta_x U_{i,j}^n U_{i,j}^n + \left( \frac{\Delta t}{2\Delta y} \right) \delta_y U_{i,j}^n U_{i,j}^n$$

where  $(i, j)$  and  $n$  are, respectively, the indices for space  $(x, y)$  and time and

$$\delta_x^2 U_{i,j}^n = U_{i+1,j}^n - 2U_{i,j}^n + U_{i-1,j}^n;$$

$$\delta_y^2 U_{i,j}^n = U_{i,j+1}^n - 2U_{i,j}^n + U_{i,j-1}^n;$$

$$\delta_x U_{i,j}^n = U_{i+1,j}^n - U_{i-1,j}^n$$

$$\delta_y U_{i,j}^n = U_{i,j+1}^n - U_{i,j-1}^n$$

## 2. Scenario

In the context of GPA, such transport phenomena can be visualized in terms of a continuous symmetry breaking during the convection diffusion evolution.

The generic scenario we assume in this paper is a hybrid diffusion process (HDP) composed by three sequential, and time dependent, phenomenological regimes ( $R_1$ ,  $R_2$  and  $R_3$ ):

$R_1$ : we consider a stochastic process measured by means of the  $U(x, y, \tau)$  where  $\tau$  is a Birkhoff characteristic

time scale (i.e.,  $U(x, y, \tau) = U(x, y)$  when  $\tau \rightarrow \infty$ ). In this regime the mean-squared energy variation of the system is given by:  $\langle U(\tau) \rangle^2 = D_q \tau^\alpha$ , where  $D_q$  is the generalized diffusion coefficient and  $\alpha$  is the anomalous exponent. Such distribution can characterize, by means of the value of the statistical index  $\alpha = f(q)$ , if the diffusion is normal or anomalous [6]. Thus, in this first regime of the process the generation of 2D-cumulative energy distributions occurs, and we can use the following notation to characterize these distributions  $U_q(x, y)$ .

$R_2$ : After the fully development of the first regime, we consider that a possible intrinsic global nonlinear instability occurs and a transition to transport dynamics of the envelope  $U_q(x, y)$  takes place in a time scale  $t \ll \tau$ .

$R_3$ : Due to the instability in  $R_2$ , a very fast convection diffusion of the envelope  $U_q(x, y)$  develops according to the 2D Burgers' equation. Note that the 2D cumulative energy distribution  $U_q(x, y)$  is the initial condition to this last regime, so that we use, for this last regime, the notation  $U_q(x, y, t)$ .

Our principal aim, in this work, is to analyze the spatial-temporal  $R_3$  regime described above for different initial conditions distributions. For this, we have performed solutions for Burgers' equation in two spatial dimension obtained by means of the 4<sup>th</sup> order Runge-Kutta scheme. The boundary conditions for all cases were chosen as  $U(0, y, t) = U(x, 0, t) = U(50, y, t) = U(x, 50, t) = 0$ . To be consistent with the first regime ( $R_1$ ), the initial conditions were given by Gaussian and non-Gaussian distributions obtained from the *generalized thermostatistics formalism* [5]. For physical purposes (mainly, long-range correlations), from [6], the generalized distribution is given by:

$$U(S_{i,j}) = \frac{(1 - \beta(1-q)S_{i,j}^2)^{\frac{1}{1-q}}}{Z_q} \quad (1)$$

where  $Z_q$ , for  $1 < q < 3$ , is the normalization factor given by:

$$Z_q = \left( \frac{\pi}{\beta(q-1)} \right)^{\frac{1}{2}} \frac{\Gamma\left(\frac{3-q}{2(q-1)}\right)}{\Gamma\left(\frac{1}{q-1}\right)} \quad (2)$$

The parameter  $\beta$  is a Lagrange parameter associated with the temperature [6]. Many distributions,  $U(S_{i,j}) \beta^{1/2}$  versus  $S_{i,j} \beta^{1/2}$ , for typical values of  $q$ , can be obtained from Equation 1. In Figure 1, some examples of the probability distribution derived from Tsallis statistics, for some values of the exponent  $q$ , are shown. When  $q = 1$ , it corresponds to a Gaussian distribution and it's important to note the long-tailed power-law distributions for  $q > 5/3$ .

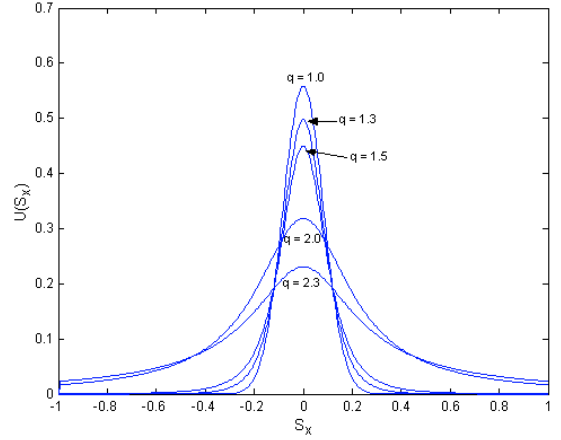


Figure 1. Some profile of 1D probability distribution derived from Tsallis statistics.

Figure 2 shows an envelope evolution for the initial condition  $q = 1$ .

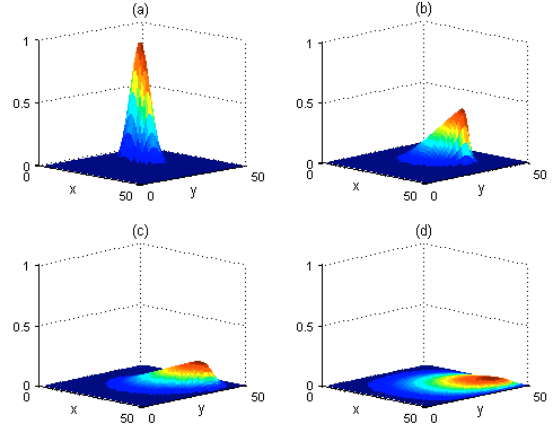


Figure 2. Four envelopes for  $q = 1$  corresponding to: (a) frame 1; (b) frame 5; (c) frame 15; (d) frame 50.

### 3. Space Parameterization

The energy  $U$ , in our approach, is distributed in an arbitrary non-linear space,  $S_{x,y}$ , according to a probability density function. And as described in  $R_3$ , of our scenario, this energy envelope  $U$  starts to diffusing in this space. As an example, when the space  $S_{x,y}$  is parameterized according to the real physical space  $x, y$  in a Cartesian coordinates, this scenario is close to the geophysical energy dissipation accumulated in a 2D tectonic plate during a earthquake.

In order to show the response of the system to the initial condition variability the parameter  $q$  was varied. Regarding anomalous diffusion, as the main process during the first regime  $R_1$ , the case  $q < 1$  is irrelevant [5]. Therefore, the focus is on the case  $1 < q < 2$ . For the two

dimensional case one finds the following sub-regimes: (a) the interval  $1 < q < 1.5$  corresponds to a transition to a superdiffusive process, and (b) the interval  $1.5 \leq q < 2$  an anomalous superdiffusion is obtained [6].

In Figure 3, we show the temporal evolution of spatially extended pattern  $U_q(x, y)$  visualized as normalized intensity contours:  $U_1(x, y)$  ( $R_1$  as a gaussian normal diffusion),  $U_{1.3}(x, y)$  ( $R_1$  as a non-gaussian normal diffusion),  $U_{1.5}(x, y)$  ( $R_1$  as a quasi-superdiffusive regime) and  $U_{1.9}(x, y)$  ( $R_1$  as a fully superdiffusive regime).

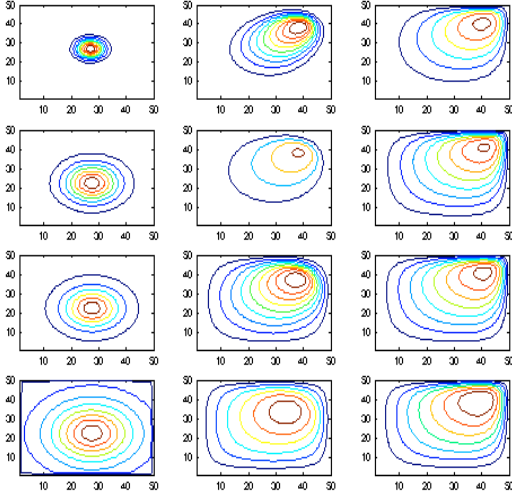


Figure 3. Pattern evolution varying  $q$ : the top sequence of three frames is for  $q = 1.0$  (Gaussian); the second sequence from the top shows the pattern evolution for  $q = 1.3$ ; the third sequence from the top is for  $q = 1.5$  and the bottom sequence is for  $q = 1.9$ .

#### 4. Gradient pattern analysis

The GPA formalism performs numerical investigation of spatio-temporal complex patterns by using computational operators such as AAF (Asymmetric Amplitude Fragmentation) [4] and CEF (Complex Entropic Form) [6]. Usually, the classical measures of complex variability doesn't take into account the directional information contained in a vector field. On the other hand, characterization of symmetry breaking in the gradient field of a given dynamical matrix has been shown to be a useful tool to understand complex regimes as intermittence and localized turbulence [7].

The spatially extended pattern  $U_q(x, y, t)$  in two dimensions  $(x, y)$  is represented by the matrix amplitude distribution  $P_M = L^{N \times N} \{U(x, y) \mid i, j \in \mathcal{R}\} \equiv U$ , essentially a square matrix of amplitudes if the two dimensions are discretized into  $N$  values each. The local fluctuation of the

spatial pattern is characterized by its gradient vector at each mesh-point in the two-dimensional space. The gradient field specifies quantitatively the variations at a given point and it is the proper quantitative indicator of the changes in the distribution of the snapshots, i.e., an indicator of the variability pattern. In other words, in this approach, the relative values of the amplitude in the matrix are dynamically relevant, rather than their absolute values.

In Figure 4, we show a set of possible profiles of local snapshot fluctuation. For a given snapshot  $U_i$  we characterize the amplitude fluctuation by means of  $U_+ = |U_i - U_{i+1}|$  and  $U_- = |U_i - U_{i-1}|$ . We call symmetric fluctuations when  $U_+ = U_-$  (examples 4a, 4b and 4c) asymmetric fluctuations otherwise (examples 4d, 4e and 4f) [9].

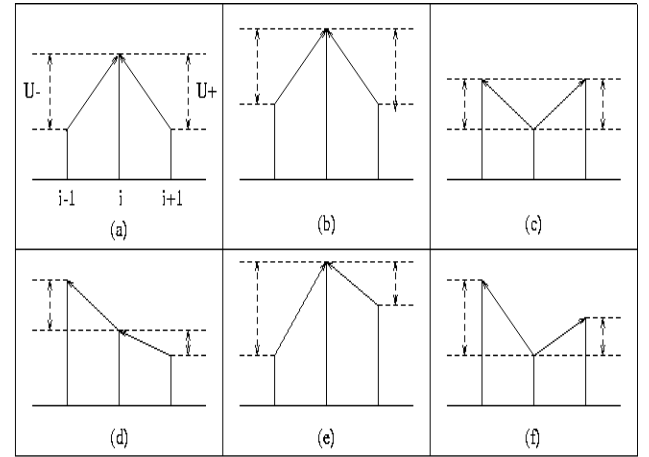


Figure 4. Symmetric and asymmetric possible profiles of local snapshot fluctuation.

Gradient Asymmetric Field: Removing every pair of symmetric vectors from the  $\nabla U$  field, we will be generating a field with  $L$  vectors (surviving to this operation), all of them vectorially asymmetric, represented by the set  $A^L(E) = \{L_i + L_j \neq 0 \text{ for all } i \neq j\} \varepsilon$ .

The two operators used to characterize both the amplitude patterns of the system allow to quantify symmetry breaking (AAF) and phase disorder (CEF) in the gradient field. The Asymmetric Amplitude Fragmentation (AAF) operator verifies the distribution of vectors in the gradient field and eliminates those with the same magnitude, within a small error, and vectorial symmetry (those with opposite orientations). The total number of the asymmetric vectors is denoted by  $L$  and connecting the middle points of the  $L$  vectors with  $I$  straight lines, we obtained a triangulation field  $T(I, L)$ . The difference  $I - L$  normalized by  $L$  is a measure of the asymmetry, called Asymmetric Amplitude Fragmentation, also given by:

$$F_a \equiv \frac{I - L}{L}, \quad (I \geq L \neq 0) \quad (3)$$

The Complex Entropic Form (CEF) operator is obtained from a generalization of the concept of degeneracy, given by the multinomial coefficient formula, and normally used to deduce the expression of Shannon's entropy of positive scalar fields. Considering the gradient matrix of the amplitude envelope, the CEF is given by [2]:

$$S_Z = -\sum_{k,l} \frac{Z_{k,l}}{Z} \ln\left(\frac{Z_{k,l}}{Z}\right) \quad (4)$$

where  $Z_{k,l} = \nabla U$  and  $Z = \sum_{k,l} Z_{k,l}$

Clearly,  $S_Z$  is a complex number that can be read as  $S_Z = |S_Z| e^{i\phi_s}$ , where  $|S_Z|$  is the module and  $\phi_s$  is the phase. The CEF operator displays interesting properties, several of which it shares with Shannon's entropy. In particular, it is possible to verify that  $S_Z$  is invariant under rotation and scaling of the vector field. Besides of being a measure of regularity, this operator permits to quantify the degree of phase disorder associated with a given gradient field. The phase  $\phi_s$  plays an important role in the analysis of pattern changing frequency in the amplitude domain.

A new tool to characterize the 2D-pattern dynamics obtained from spatio-temporal non-linear systems is plotting patterns signature in the space Asymmetric Fragmentation x Phase.

Figure 5 shows the signature of four different initial conditions ( $q = 1.0$  (Gaussian),  $q = 1.3$ ,  $q = 1.5$ ,  $q = 1.9$ ). It's possible to verify that different patterns occurs for these different initial conditions. In the case of  $q = 1$ , the pattern evolution occurs in a spread way (Figure 5.a). For the  $q = 1.3$  (Figure 5.b), we can observe a kind of cluster on the evolution pattern, which becomes more intensive on the superdiffusive regimes. On these initial conditions (Figures 5.c and 5.d), there is no more the spread observed in the others regimes.

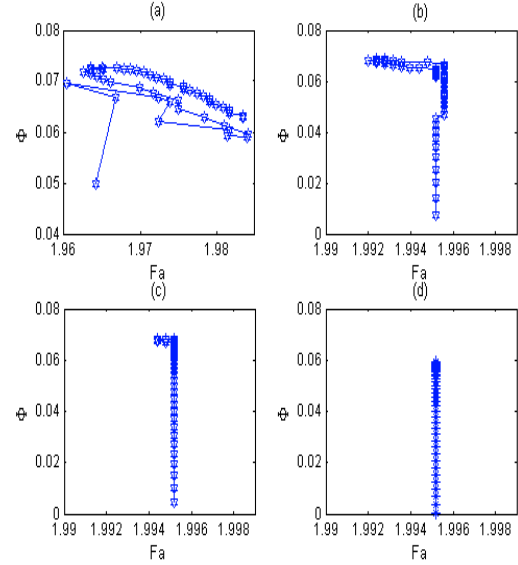


Figure 5. Phase diagram (Fa versus  $\phi_s$ ) for  $q = 1$  (a), for  $q = 1.3$  (b),  $q = 1.5$  (c), and  $q = 1.9$  (d).

The spread that occurs on the pattern evolution varying  $q$  is given by:

$$D = (\text{Var}(Fa) * \text{Var}(\phi_s))^{1/2} \quad (5)$$

In Figure 6, this measure is plotted varying the initial condition from  $q = 1$  to  $q = 1.9$ . One can see the transposition between the Gaussian initial condition to a transition to superdiffusive regime and to superdiffusive regime.

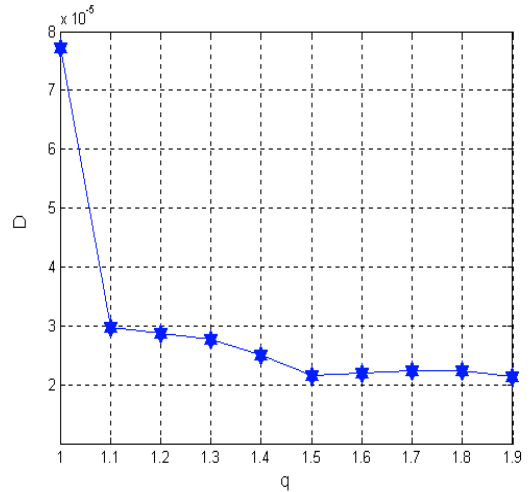


Figure 6. Pattern evolution signatures (Fa versus  $\phi_s$ ) dispersion for  $q$  varying from 1.0 to 1.9.

## 5 Concluding Remarks

The analytical approach introduced in this paper will be useful for characterization of spatio-temporal regimes in

extended systems where there is no information about the initial conditions. The methodology, using the gradient pattern analysis, is to characterize the processes  $R_1$ ,  $R_2$  and  $R_3$  using only few frames observed during the process  $R_3$ .

In particular, the HDP proposed here can play a fundamental role in the energy diffusion mechanism of a wide class of systems: impulsive bursts in plasmas [8]; transport in heterogeneous media, such as Lagrangian drifters in the ocean flow [9], nonuniform distribution of strengths over a fault plane that generates earthquakes [10] and the asset price change after a bubble financial rupture [11].

## References

- [1] Rosa, R.R.; Sharma, A.S. & Valdivia, J.A., "Characterization of asymmetric fragmentation patterns in spatially extended systems", *Int. J. of Modern Physics C*, Word Scientific Publishing Company, 1999, 10 (1), 147-163.
- [2] Ramos, F.; Rosa, R.R.; Rodrigues Neto, C. & Zanandrea, A., "Generalized complex entropic form for gradient pattern analysis of spatio-temporal dynamics", *Physica A*, Elsevier, 2000, 283, 171-174.
- [3] Rosa, R.R.; Pontes, J.; Christov, C.I.; Ramos, F.; Rodrigues Neto, C. ; Rempel, E.L. & Walgraef, D., "Gradient pattern analysis of Swift-Hohenberg dynamics: phase disorder characterization", *Physica A*, Elsevier, 2000, 283, 156-159.
- [4] Rodrigues Neto, C. ; Rosa, R.R; & Ramos, F., "Pattern characterization: a case study in osmosedimentation", *Int. J. of Modern Physics C*, Word Scientific Publishing Company, 2001, 12 (8), 1261-1269.
- [5] Tsallis, C., "Non-extensive thermostatistics: brief review and comments", *Physica A*, Elsevier, 1995, 221, 277-290.
- [6] Zanette, D.H., "Statistical-thermodynamical foundations of anomalous diffusion", *Brazilian J. of Physics*. 1999, 29 (1), 108-124.
- [7] Rosa, R.R; Sharma, A.S. & Valdivia, J.A., "Characterization of localized turbulence in plasma extended systems", *Physica A*, Elsevier, 1998, 257(1-4), 509-514.
- [8] Sawant, H.S., Rosa, R.R; Ceccato J.R. & Gopalswamy, N. "Source parameters for impulsive bursts observe in the Range 18-23 GHz", *Solar Physics*, Kluwer Academic Publ., 1997, 171(1), 155-159.
- [9] Assireu, A.T., Rosa, R.R.; Vijaykumar, N.L.; Lorenzetti, J.A., Rempel, E.L.; Ramos, F.; Abreu Sá, L.D.; Bolzan, M.J.A. & Zanandrea, A., "Gradient pattern analysis of short nonstationary time series: an application to Lagrangian data from satellite tracked drifter", *Physica D*, Elsevier, 2002, 168-169, 397-403.
- [10] Bak, P., & Tang, C., "Earthquakes as a Self-Organized Critical Phenomenon", *Journal of Geophysical Research*, 1989, 94(B11), 15635-15637.
- [11] Mattedi, A.P.; Ramos, F. M.; Rosa, R.; De Marchi, M.M. & Bins, L.S., Análise Físico-Estatística do índice "S&P500" Futuro: um estudo de caso para 1998-2001. *I Workshop dos Cursos de Computação Aplicada do INPE*, São José dos Campos, 2001, 100-102.
- [12] Rosa, R.R, "A semi-implicit routine to solve non-linear PDE's in two dimensions", *XVIII CNMAC*, Paraná, 1995.

**Acknowledgment:** This work was supported by FAPESP-Brazil (Proc. 97/13374-1), CAPES-Brazil and CNPq-Brazil